Structural reliability analysis of secondary hull detail

S.K. Kleivane & B.J. Leira
Norwegian University of Science and Technology, Department of Marine Technology, Trondheim, Norway

ABSTRACT: A reliability model for analyzing the possible occurrence of crack propagation of a secondary structural detail is developed. Vibration response due to engine excitation is formulated by a stochastic model based on analysis of a general cargo hold structure. Engine speed and cargo tank filling level are taken as stochastic variables. A limit state is formulated based on a threshold stress intensity factor for crack growth and expresses the possible occurrence of fatigue crack propagation. Failure probabilities are estimated by Monte Carlo simulations and reliability approximation methods (FORM/SORM). The adequacy of the applied stochastic model for vibration is evaluated and the robustness of the estimated failure probabilities is assessed. One main remark is that the reliability-based design of secondary details may lead to an improvement in the fatigue capacity of the detail.

1 INTRODUCTION

1.1 *Ship hull vibration*

One constant concern for ship designers and operators is to reduce ship vibrations and the hull structure will be exposed to different excitation types. Excessive ship vibration can cause fatigue failure of local structural details and welded components are especially exposed to fatigue failure due to the construction and presence of the weld itself. The vibrations are observed at both global and local levels and due to this feature, there does not exist one general method to solve any kind of vibration problems arising onboard a ship. In addition, fatigue crack growth is a highly complex and uncertain phenomenon. These aspects encourage a reliability-based formulation for assessing hull vibration and fatigue crack growth. Over the decades, several major sources of ship hull vibration have been identified and broadly investigated. One of these sources is vibration excitation from the marine diesel engine.

1.2 *Engine excitation*

The two-stroke low-speed diesel engine is identified as a substantial source of hull vibration. These engines have been favored as the main engine for ocean-going vessels due to their high efficiency and reliability and low price (MAN Energy Solutions, 2020; Bukovac et al., 2015). The engine can directly cause vibration through dynamic forces transmitted through its foundations and supports (American Bureau of Shipping, 2021). In addition, due to their invariably large size, they are typically bolted directly onto the ship structure leading to the engine vibration being fully transmitted into the hull structure. When determining the source of vibration, it is necessary to establish the frequency of excitation and relate this frequency to the shaft rotational frequency by determining the number of oscillations per shaft revolution, which is typically expressed as revolutions per minute (rpm) (American Bureau of Shipping, 2021). The low-speed engine generally has an operating speed range somewhere between 70 to 130 rpm. There is typically no requirement for speed reduction arrangement or reduction gear, referred to as direct drive to the propeller shaft. Direct drive propulsion systems have a fixed-pitch propeller, and the propeller rpm remains the same as the engine rpm.

Looking back just one decade, a rather limited number of references to machinery-induced vibration in ship hull structures existed. However, the topics came undoubtedly into focus after the introduction of the so-called Comfort Class requirements. These requirements were first introduced by DNV in 2011 and later by Lloyds' Register and Bureau Verities, and other classification societies later (International Ship and Offshore Structures Congress (ISSC), 2018; DNV, 2011). They provided stricter requirements for vibration, noise, and indoor climate onboard ships, which forced the maritime community to pay additional attention to machinery-induced vibration, especially vibration generated by the marine diesel engine.

In modern engine manufacturing, advanced numerical simulation and calculation techniques are used to analyze engine performance already at the design stage, taking excitation, structure, and vibration response into account. Therefore, excitation forces with all possible firing orders can be compared and analyzed, structural properties such as engine stiffness can be optimized, and dynamic simulations of the engine's vibration response can be simulated (Tienhaara, 2004). Therefore, the engine manufacturer provides the external forces and moments from engine vibration, usually tabulated in engine specifications and project guides. The forces and moments are typically reported at specific engine ratings, i.e., at specific engine speeds and powers.

2 RELIABILITY ASSESSMENT

Structural reliability assessments are used for the prediction of failure probabilities of a system at any stage during the structural life. The probability of failure may be used as a measure of safety and gives a more explicit measure than safety factors (Melchers, 1998). Ship structural systems are complex and large systems and reliability assessments may involve multiple states which usually are correlated. To analyze such a system, simplifications are introduced concerning loads, strength characteristics, responses, and the connection between the system and the components. This introduces uncertainties in addition to those already inherent in the structure.

A reliability assessment is generally described by a limit state violation: $G(\boldsymbol{x}) < 0$, where G is an appropriate limit state function. This formulation states the regions of the problem which are safe and unsafe concerning failure based on a given event, as illustrated in Figure 1.

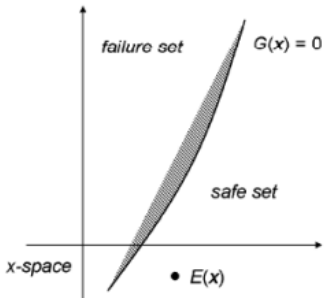

Figure 1. Limit state formulation for event $E(\boldsymbol{x})$ (DNV, 2004b).

A reliability problem has the general form:

$$p_f = P(G(\boldsymbol{x}) \leq 0) = \iint \ldots \int_{G(\boldsymbol{x})\leq 0} f_{\boldsymbol{X}}(\boldsymbol{x}) d\boldsymbol{x} \qquad (1)$$

where p_f is the failure probability, $G(\boldsymbol{x}) \leq 0$ is the limit state formulation, and $f_{\boldsymbol{X}}(\boldsymbol{x})$ is the joint probability density function (pdf) for the vector $\boldsymbol{x}$ of basic variables (Moan, 2009). This equation cannot generally be solved analytically. Reliability approximation methods and Monte Carlo simulations are extensively used for solving such problems.

2.1 *Approximation methods*

The first-order reliability method (FORM) and the second-order reliability method (SORM) are extensively used for assessing failure probabilities. These methods approximate the integral in equation (1). The fundamental idea for both methods is to transform the problem from a given space, say x, to the standard normal space, denoted u. This approximates the surface of the boundary of the area where the specific event investigated is fulfilled. The integration can then be done over this approximated area (DNV, 2004b; Moan, 2009). The main difference between FORM and SORM is that FORM uses a first-order surface to approximate the event boundary, and SORM uses a second-order surface to approximate the event boundary. The two methods are illustrated in Figure 2.

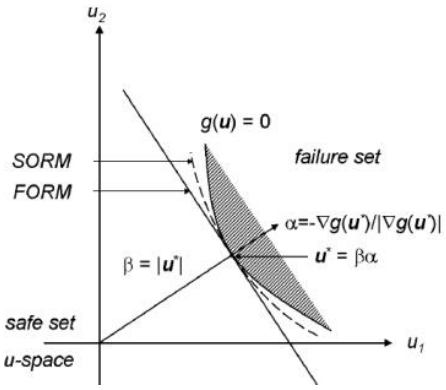

Figure 2. FORM/SORM approximation to failure surface (DNV, 2004a).

These approximation methods use the Rosenblatt transformation to transform the reliability problem to the space of standard normal variables. The Rosenblatt transformation is a general method for transforming non-normal random variables into equivalent independent Gaussian distributed variables (Moan, 2009).

2.2 *Monte Carlo simulation methods*

The Monte Carlo simulation methods construe probability as relative frequency and artificially simulate several experiments by randomly sampling and judging the results (Moan, 2009; Melchers, 1998). To use these methods the stochastic variables must be established or chosen in advance and then a systematic method for numerical sampling of the basic variables is established (Melchers, 1998). The simplest method is the so-called crude Monte Carlo method. This is the most direct method; however, it is not the most efficient method. The method has a severe penalty with a slow convergence (of the standard deviation).

Therefore, variance reduction techniques have been introduced to make the simulation method more cost-effective (Moan, 2009). One such method is importance sampling, which uses known information about the problem to constrict the simulation to interesting domains. The basic formulation for both methods is based on the same general principle, using an indicator function which is evaluated at each sample point and gives a value, typically 1, if a failure occurs.

2.3 *Proban*

The reliability assessment is conducted using Proban, developed by DNV. Proban is a general-purpose probabilistic analysis program that covers calculation needs, for example in structural reliability (Tvedt, 2006). A wide set of different statistical and probabilistic problems encountered in engineering can be evaluated by this program through a variety of approximation and simulation methods. This makes the program ideally suited for structural reliability analyses (DNV, 2004b).

3 METHODOLOGY

3.1 *Main engine*

A finite element (FE) model of an engine is not available for the author at this stage, but through contact with an engine manufacturer, data for external forces and moments for an engine typically used in tankers are provided. The engine is a 6-cylinder MAN B&W G50ME-C9.5. Ships installed with a 6-cylinder main engine usually have moment compensators to mitigate the critical 2nd external vertical inertia moment, which is the most critical source of excitation from the engine. This is assumed for the tentative vessel, therefore, only guide force couples are investigated as an excitation source. These forces and moments are a result of the combustion process in the engine. The provided data has no connection to the real operation of a ship but is given for a specific engine rating for simulation purposes. The guide force couple moments for the specific engine are given in Table 1 for five different rpms used in the vibration analysis.

Table 1. External guide force couple moments

Guide force H-moment [kNm]					
Order	80rpm	83rpm	85rpm	87rpm	90rpm
6	825.9	826.9	827.6	828.4	829.5
12	65.7	65.7	65.7	65.7	65.7
Guide force X-moment [kNm]					
Order	80rpm	83rpm	85rpm	87rpm	90rpm
2	241.5	226.8	215.8	204.5	188.7
3	524	492.1	468.1	443.7	409.2
4	270.3	268.2	266.6	265	262.8
8	83.3	83.3	83.3	83.3	83.3
9	144.7	144.7	144.7	144.7	144.7
10	36.6	36.6	36.6	36.6	36.6

We see that some of the moments are the same for the different rpms, however, the order frequency will change for each order and rpm. The engine excitation frequencies are calculated as engine speed times order number and divided by 60 to go from rpm to Hz.

3.2 *Cargo arrangement*

The modelling of cargo in tanks is solely concerned with simulating the effect of additional mass on the dynamic behavior of the hold structure. Hydrodynamic aspects, such as sloshing and slamming, due to the motion of the cargo are not taken into consideration. The cargo distribution along the ship length will directly influence the global hull bending and shearing and the stresses in the local hull structures. When only evaluating the filling level in the tanks, it is assumed that as more volume in the tanks is filled, the lower the natural frequencies of the structure will be due to the increased mass.

The cargo can be distributed in various configurations. A homogeneous or alternating loading condition is considered a ship's full load condition. An alternating load condition is shown in Figure 3, and the scenario seen in this figure may be considered a worst-case scenario when only taking the tank wall's added mass and vibration aspects where a secondary structural detail is attached. This configuration will be analyzed in the work presented here.

Figure 3. Alternating load configuration (IACS, 2018).

3.3 *Stochastic variables*

The engine speed and cargo tank filling level are taken as stochastic variables. Engine speed influences the forces and moments produced by the engine. This is because the external forces and moments are influenced by engine speed (oscillating masses) and by gas excitation (cylinder pressure). The assumption of a normal distribution is based on research by Adland et al. (2020) on a framework for the estimation of the fuel consumption-speed curve for ships, where a large data set of 16 crude oil tankers where investigated. The attention is restricted to speed intervals between 6 and 16 knots, where the vessels are sailing in the open sea in laden condition. The vessel speed is then approximately normally distributed with a mean of 12.1 knots (Adland et al., 2020) Further, it can be

expected that the ship's speed (in knots) is roughly linear with the shaft rpm (Lakshmynarayanana and Hudson, 2017). Based on this, the mean and standard deviation of the engine rpm for the normal distribution description can be obtained. Based on this the following distribution shown in Figure 4 is found for the engine speed, where the mean and standard deviation is obtained using basic formulas in statistics for normal distribution.

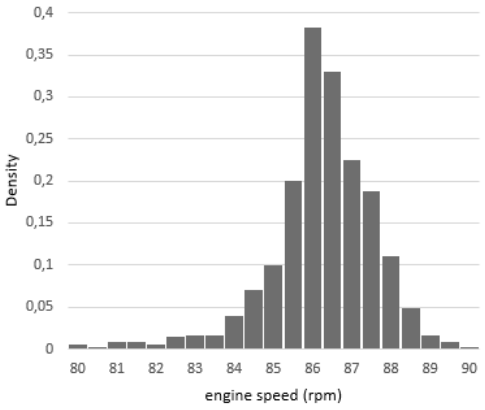

Figure 4. Distribution of engine speed in rpm.

The tank filling level is assumed to be uniformly distributed since it only changes in the z-direction (height of cargo in the tanks). This is to some extent reasonable since no hydrodynamic aspects of the cargo liquid are considered and the cargo in this case is modelled as a solid body. The mean and standard deviation for the uniform distribution of filling levels is obtained directly from Proban, where it is calculated by basic statistical formulas for uniform distribution. The characteristics of the stochastic variables are given in Table 2.

Table 2. Stochastic variables

Variable	Engine speed	Filling level
Description	X	Y
Distribution	Normal	Uniform
Range	80 – 90 rpm	0 – 100 %
Mean	86.1	50
Standard deviation	1.1	28.9

3.4 *Vibration analysis*

The vibration response is evaluated through acoustic harmonic vibration analysis in Ansys Workbench. A general cargo hold model is analyzed with engine excitation implemented as moments acting on the aft end of the structure. The engine structure is implemented as a point mass to simulate the mass of the engine block. The acoustic module considers the additional mass of the cargo, where the interaction between the cargo and the tank wall is implemented through a fluid-solid interface. The cargo hold model consists of ½ + 1 + ½ hold units, shown in Figure 5 for the case of 75% volume filling level in the tanks.

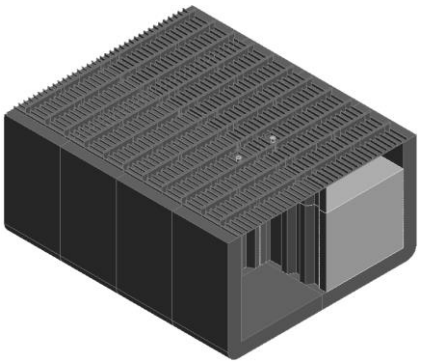

Figure 5. General cargo hold model with ½ + 1 + ½ hold units.

The model is analyzed with five different engine speeds ranging from 80 to 90 rpm, and five different filling levels, given in volume percentage of tank filling from 0 to 100%. This provides data sets for fitting a functional representation to the vibration response. As presented in Table 2, the engine speed will be given a normal distribution in the probabilistic analysis, and the filling level is assumed uniformly distributed with statistically even weighting. The secondary structural detail analyzed is the pipe stack support, seen in Figure 6.

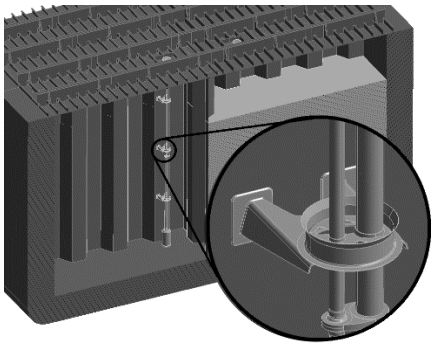

Figure 6. Pipe stack support.

The number of nodes and elements of the hold model are given in Table 3 for the different filling levels. The structural parts are steel with a density of 7850 kg/m3, except the cargo hold pump head which is given a density of 625 kg/m^3. The hydraulic pipe has distributed mass of 130kg to simulate the additional mass of hydraulic oil. The structural parts are modelled with solid elements and given a tetrahedron mesh. The cargo is simulated as water and meshed with a sweeping method. The boundary conditions are implemented according to DNV (2021b) Class Guideline for finite element analysis.

Table 3. Number of nodes and elements of FE model

Filling level [%]	Nodes	Elements
0	1252199	705740
25	1331057	729599
50	1214706	577286
75	1330825	732362
100	1326467	731348

Vibration response is evaluated as hot spot stress in the welded connections between the support and the tank wall. Stress is considered because it is a driving force for fatigue crack propagation. The hot spot stress is derived according to recommended practice from DNV (2021a) for modelling with solid elements with the weld included in the model. The hot spot stress can be taken as the stress at the read-out point 0.5 *t* away from the weld toe, where *t* is the thickness of the plate. The hot spot stress is then derived as:

$$\Delta\sigma_{HS} = max\begin{cases} 1.12\sqrt{\Delta\sigma_{\perp}^2 + 0.81\Delta\tau_{\parallel}^2} \\ 1.12\alpha|\Delta\sigma_1| \\ 1.12\alpha|\Delta\sigma_2| \end{cases} \quad (2)$$

where α is a factor which depend on what type of class the detail is defined as (ref. DNV-RP-C203 Table A-3), and $\Delta\sigma_1$ and $\Delta\sigma_2$ are principal stresses calculated as:

$$\Delta\sigma_{1,2} = \frac{\Delta\sigma_{\perp}+\Delta\sigma_{\parallel}}{2} \pm \frac{1}{2}\sqrt{(\Delta\sigma_{\perp} - \Delta\sigma_{\parallel})^2 + 4\Delta\tau_{\parallel}^2} \quad (3)$$

3.4.1 *Functional representation*

A functional representation of the vibration response is constructed based on the response data. One function is fitted to each of the stochastic variables and the final expression is taken as the product of these two functions. This is then assuming the variables are uncorrelated. The functional representation will be on the form:

$$f_S(x, y) = f_X(x) \cdot f_Y(y) \quad (4)$$

3.5 *Limit state formulation for crack growth occurrence*

The limit state is formulated as the potential occurrence of crack propagation in the local structural detail. A fatigue limit, S_l, may be defined, below which there is no fatigue damage. A useful approximation for a three-dimensional surface crack is to assume a semi-elliptic shape (Berge and Ås, 2017), with depth *a* and surface length 2*c* as seen in Figure 7.

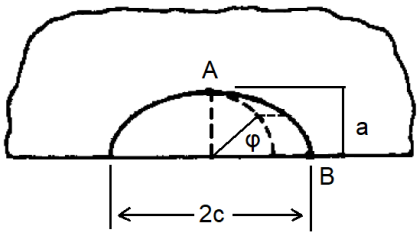

Figure 7. Semi-elliptical surface crack (Newman and Raju, 1981).

The fatigue limit is established based on a recommended fatigue crack growth threshold stress intensity factor (SIF) for welded components and SIF calculations by Newman and Raju (1981). They established an empirical expressed for the SIF based on finite element results:

$$K = S\sqrt{\pi\frac{a}{Q}}F \quad (5)$$

where *K* is the SIF, *S* is stress, *a* is crack size, *F* is a form factor and *Q* is the shape function for an ellipse, which can be approximated as:

$$Q = 1 + 1.464\left(\frac{a}{c}\right)^{1.64} \quad (6)$$

A recommended threshold value for steel is $\Delta K_{th} = 63\text{MPa}\sqrt{\text{mm}}$ (British Standard, 2005), and the fatigue limit can then be expressed as:

$$S_l = \frac{\Delta K_{th}}{\sqrt{\pi\frac{a_i}{Q}}F} \quad (7)$$

The form factor is dependent on the external geometry, crack length, crack geometry and load configuration. To evaluate this factor, the initial crack size must be established. However, it is difficult to estimate the initial crack size in welded structures and different values are given in the literature (e.g., British Standard, 2005; Hobbacher, 2009). Therefore, different crack sizes are considered to evaluate the effect of initial crack size on the fatigue limit.

The geometry function is established based on the SIF calculation results by Newman and Raju (1981), where they have established graphs of an equivalent form factor. However, the initial cracks may be considered small compared to the overall geometry and it may then be sufficiently accurate to assume infinite plate solutions (Berge and Ås, 2017), which means the form factor is equal to 1.

Concerning the avoidance of crack propagation, it is challenging to establish an exact criterion for an acceptable probability of failure. This needs to be based on several different parameters and aspects (such as experiments and experience). Due to a lack of information, no specific criterion can be set herein. However, a failure probability from 1-5% may be argued as not critical.

The limit state for failure probability estimation is now formulated as:

$$G(x) = S_l - f_S \leq 0 \quad (8)$$

where f_S is the local stress response at the structural detail under consideration.

4 RESULTING RELIABILITY MODEL

4.1 *Vibration aspects*

The vibrational data set based on five different rpms and filling levels is a relatively small set of data. However, due to the computational demand for each simulation, a compensation between simulation time and data points simulated was necessary.

Preliminary investigations of vibration response due to main engine excitation alone give stress levels which may be considered as not critical. The global vibration and the vibration levels in the cargo tanks themselves are well below requirements given by different recommendations (e.g., International Organization for Standardization, 2016; American Bureau of Shipping, 2021). From a design point of view, analyzing the fatigue capacity of a secondary detail; the design should be aimed to withstand normal to critical vibration levels. Due to limitations in the author's possible modelling opportunities at this stage, no consideration is made of hydrodynamic loads and loads from the propeller or other possible excitation reinforcements of the ship. It may therefore be reasonable to assume that vibration from the main engine alone will not be critical in the mid-region ship structure.

To test the developed stochastic model further, a reinforcement factor for the ship can be assumed. Essentially this consists of scaling the global vibration response toward critical limits to investigate the fatigue capacity of the local detail. The main aspect herein is to test the integrity of the developed stochastic model for the possible occurrence of crack propagation.

4.2 *Response function*

Due to a relatively small vibration response data set, it is aimed to fit well-established functional representations to the data. The curve fits are evaluated by their goodness of fit statistics: the sum of squares due to error (SSE), the R-square, and the root mean squared error (RMSE). For a fit useful for prediction, the SSE and RSME should be as close to zero as possible, and the R-square should be as close to 1 as possible.

The curves are fitted based on the average hot spot stress in the middle support, which experiences the most significant stresses. For fitting the engine speed curve, the responses from the different filling levels are averaged at each rpm. For fitting the filling level curve, the responses from the different rpms are averaged for each filling level.

The X-variable (engine speed) is fitted to a Fourier function with the following form:

$$f_X(x) = 6.54 + 3.12\cos(0.26x) - 1.30\sin(0.26x) \quad (9)$$

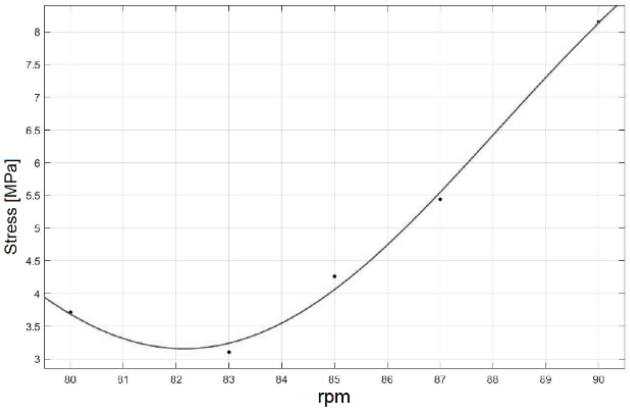

Figure 8. Fitted curve for X-variable.

The fit is plotted in Figure 8, with the goodness of fit statistics given in Table 4.

Table 4. Goodness of fit statistics for X-variable.

Parameter	Value
SSE	0.073
R-square	0.995
RMSE	0.269

The Y-variable (filling level) is fitted to a Gaussian function on the following form:

$$f_Y(y) = 13.49 \cdot e^{-\left(\frac{y-96.61}{33.12}\right)^2} \quad (10)$$

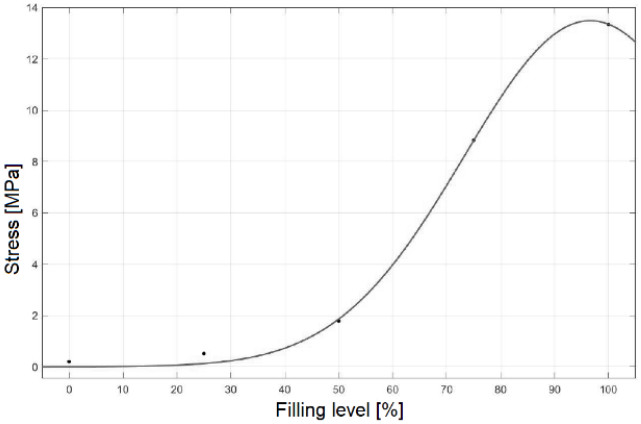

Figure 9. Fitted curve for Y-variable

The fit is plotted in Figure 9, with goodness of fit statistics given in Table 5.

Table 5. Goodness of fit statistics for X-variable.

Parameter	Value
SSE	0.193
R-square	0.999
RMSE	0.312

The resulting stochastic model for vibration response becomes:

$$f_S(x,y) = (6.54 + 3.12\cos(0.26x) - 1.30\sin(0.26x)) \cdot \left(13.49 \cdot e^{-\left(\frac{y-96.61}{33.10}\right)^2}\right) \quad (11)$$

The goodness of fit statistics for the fitted functions are to some extent satisfactory, however, with a possibility of improvements. Especially for the RMSE parameter, which is an estimate of the standard deviation of the random component in the data. Further improvement of the model will give a fit better for prediction. Improved functional representations may be achieved by, for instance, having a larger vibration data sample for curve fitting. However, both SSE and RMSE for both functions are in the vicinity of zero and the R-square for both fits is close to 1. Accordingly, some integrity of the stochastic model is achieved.

The assumption of uncorrelated variables is to some extent reasonable as the ship's speed is assumed to be determined based on the voyage, together with environmental conditions, and not related to the amount of cargo being transferred.

4.3 *Failure probability estimation*

Table 6 summarizes the different initial crack sizes investigated, with their corresponding form factor and their calculated maximum allowable stress before crack propagation occurs.

Table 6. Initial crack sizes and corresponding limit stress S_l

Initial crack [mm]		F [-]	S_l [MPa]
a_i	c_i		
0.2	0.5	1.0	91
0.3	0.5	1.0	82
0.4	0.8	1.0	68
0.5	1	1.0	60
0.6	1	0.95	61

Based on the established values, the approximation of assuming a constant form factor equal to 1 may be valid here, meaning it is reasonable to say that the crack size is considered small compared to the overall geometry. However, here it is assumed bending loading is the dominant loading for the pipe stack support. The loading condition will be more complex, consisting of combinations of different loading types. In addition, the values for the form factors are based on graphical representations of typical results for SIF solutions and there will be uncertainties associated with the read values.

The failure probability calculations are conducted with the normalized response functions to obtain correct units in the stress calculations. The reference response is for the case with 50% filling level and engine speed of 85 rpm. Table 7 summarizes the calculated failure probabilities.

Table 7. Failure probabilities

Initial crack		S_l	p_f [%]			
a_i	c_i		MC	DSPS	FORM	SORM
0.2	0.5	91	0.00	0.00	0.00	0.00
0.3	0.5	82	0.01	0.01	0.03	0.01
0.4	0.8	68	0.56	0.57	1.26	0.51
0.5	1	60	2.49	2.42	4.65	2.33
0.6	1	61	2.06	2.07	4.05	1.96

* MC: crude Monte Carlo

* DSPS: design point simulation (importance sampling)

For a smaller fatigue limit the calculated failure probability is larger. Moreover, the failure probabilities estimated by crude Monte Carlo (MC) and importance sampling (DSPS) are similar. These two aspects are as expected and present a satisfying result for the reliability model regarding its robustness in failure probability estimation. The failure probability by SORM coincides with the MC and DSPS probability. However, the FORM probability deviates noticeably from the others. One reason for this can be that the problem's failure surface is displaying nonlinear characteristics, thus, the surface is possibly quite curved.

The calculated failure probabilities are below the specified range of 1-5%. However, values are uncertain and represent a criticism of probability calculation. Acceptable criteria and target values are difficult to establish. This means that there may be a risk of the occurrence of crack propagation and further investigations based on a continuation of this reliability framework can help improve the failure capacity of local details such as the pipe stack support investigated herein.

5 CONCLUSION

The harmonic vibration analysis is only done for combinations of five different rpms and filling levels. This may be too few points for an optimal representation of response functions. However, due to the computational demand for each vibration simulation, it was necessary to compensate between simulation time and the size of the sample. Nevertheless, the established stochastic model has achieved adequate integrity with a small set of vibration data.

The failure probability estimated by the reliability model increases for increasing crack size and decreasing fatigue limit. This gives robustness to the model since it coincides with the expected results.

Based on the functional representations for the filling level and rpm, it is seen that both variables will noticeably influence the vibration response of the local structure. A larger filling level, 50% of the tank and above, combined with RPMs in the region of the mean value and above, gives the largest responses for the structural detail. Therefore, the local components

may be exposed to vibration which over time can lead to critical fatigue crack growth. By further development of the framework presented herein, the reliability-based design of secondary details may lead to an improvement in the fatigue capacity of the detail.

6 REFERENCES

Adland, R., Cariou, P., & Wolff, F.-C. (2020). Optimal ship speed and the cubic law revisited: Empirical evidence from an oil tanker fleet. *Transportation Research Part E: Logistics and Transportation Review*, 140, 101972. https://doi.org/10.1016/j.tre.2020.101972

American Bureau of Shipping. (2021). Guidance note on Ship Vibration. (ABS). Texas, USA.

Berge, S., & Ås, S. K. (2017). Fatigue and Fracture Design of Marine Structures. *TMR4200 Compendium*.

British Standard. (2005). Guide to methods for assessing the acceptability of flaws in metallic structures. (BS 7910:2005). Retrieved from: https://www.academia.edu/33758342/Guide_to_methods_for_assessing_%20the_acceptability_of_flaws_in_metallic_structures

Bukovac, O., Medica, V., & Mrzljak, V. (2015). Steady state performances analysis of modern marine two-stroke low speed diesel engine using mlp neural network model. *Shipbuilding*, 66 (4), 57–70. https://www.researchgate.net/publication/295114070_Steady_state_performances_analysis_of_modern_marine_two-stroke_low_speed_diesel_engine_using_mlp_neural_network_model

DNV (2021a). Fatigue design of offshore steel structures, Recommended Practice, DNV-RP-C203.

DNV (2021b). Finite element analysis, *Class Guideline*, DNV-CG-0127.

DNV (2011). Rules for classification of ships: Comfort Class. Det Norske Veritas (DNV), *Special service and type addition class*. Retrieved from https://rules.dnv.com/docs/pdf/DNVPM/rulesship/2011-01/ts512.pdf.

DNV (2004a). SESAM User Manual Proban. Det Norske Veritas, DNV Software Report No.: 92-7049. Høvik, Norway

DNV (2004b). SESAM User Manual Proban Theory. Det Norske Veritas, DNV Software Report No.: 96-7017. Høvik, Norway.

Hobbacher, A. (2009). The new IIW recommendations for fatigue assessment of welded joints and components – a comprehensive code recently updated. *International Journal of Fatigue*, 31, 50–58. https://doi.org/10.1016/j.ijfatigue.2008.04.002

IACS. (2018) Guidance and Information on Bulk Cargo Loading and Discharging to Reduce the Likelihood of Over-stressing the Hull Structure, No. 46, London.

International Ship and Offshore Structures Congress (ISSC). (2018). *ISSC 2018 Technical Committee II.2 Dynamic Response*. https://doi.org/10.3233/978-1-61499-862-4-255

Lakshmynarayanana, P. A., & Hudson, D. (2017). Estimating added power in waves for ships through analysis of operational data. *2nd Hull Performance and Insight Conference*.

MAN Energy Solutions. (2020). Two-Stroke Technology. https://www.man-es.com/marine/products/two-strokeengines

Melchers, R. E. (1998). Structural reliability analysis and prediction. John Wiley & Sons.

Moan, T. (2009). Structural Risk and Reliability Analysis. Department of Marine Technology, NTNU, Trondheim, Norway.

Newman, J., & Raju, I. (1981). An empirical stress-intensity factor equation for the surface crack. Engineering Fracture Mechanics, 15 (1), 185–192. https://doi.org/https://doi.org/10.1016/0013-7944(81)90116-8

Tienhaara, H. (2004). Guidelines to engine dynamics and vibration [Technology, Wärtsilä Corporation]. https://www.maintenance.org/fileSendAction/fcType/0/fcOid/399590942962914489/filePointer/399590942964822834/fodoid/399590942964822832/Wartsila_Guideline_Dynamics_Vibrations.pdf

Tvedt, L. (2006). Proban - probabilistic analysis. *Structural Safety - STRUCT SAF*, 28, 150–163. https://doi.org/10.1016/j.strusafe.2005.03.003